RSC Advances

ROYAL SOCIETY OF CHEMISTRY

www.rsc.org/advances

ROYAL SOCIETY
OF CHEMISTRY

Journal Name

ARTICLE TYPE

Tunable nanocrystalline CoFe$_2$O$_4$ isotropic powders obtained by co-precipitation and ultrafast ball milling for permanent magnets applications

F. J. Pedrosa,[a] J. Rial,[a] K. M. Golasinski,[a] M. Rodríguez-Osorio,[a] G. Salas,[a] D. Granados,[a] J. Camarero,[a,b] and A. Bollero[*,a]

Synthesis of nanocrystalline Co-ferrite powders with tuneable magnetic properties is demonstrated by using co-precipitation and a novel flash-milling route. Milling times as short as a few minutes are reported for the first time to be sufficient to refine microstructure and to induce microstrain, which act efficiently providing a 5-fold increase in coercivity. This is achieved with no compositional change during processing, but exclusively through microstructural modification. The efficiency of this process and its feasible scalability pave the way for development of Co-ferrite powders for permanent magnet applications.

1 Introduction

During the last years, substitution of materials and innovative processing technologies in the permanent magnet industry are focused to avoid the supply risks due to mining oligopoly or speculation as well as to find efficient technological processes. It is a general consensus among the scientific community that complete substitution of rare earth-based permanent magnets in all existing technological applications is not an option in a long term, which is due to the unique combination of magnetic properties of the Nd$_2$Fe$_{14}$B phase[1,2]. However, international research efforts aim to find materials alternatives that allow optimizing the traditional indiscriminate use of rare-earth magnets, i.e. promoting a well-focused use of these magnets in technological areas where alternatives cannot match their magnetic performance (mainly in terms of miniaturization where a high magnetic performance is required in a reduced volume). The so-called maximum energy product, $(BH)_{max}$, is typically used to describe the quality of a permanent magnet[3]. This quantity provides a measure of the magnetic energy density that can be stored in the considered material and it is defined as the maximum value of $B \times H$ (B: magnetic induction; H: applied magnetic field) on the second quadrant of the B-H hysteresis loop. One of the most immediate objectives in the search of rare earth-free permanent magnets alternatives is the substitution of low-grade rare-earth bonded magnets with typical values of $(BH)_{max}$ of tens of kJ m^{-3} (depending on the amount of polymer bonding employed). However, and prior to the processing of fully dense magnets, an optimization of the initial isotropic free-standing permanent magnet powders is required. In order to achieve this goal -in particular, for the reduction of rare-earth based materials- it has been proposed to employ ferrites as a promising approach for high coercivity permanent magnet applications.[4] Coercivity is the ability to resist demagnetization, including field demagnetization from the electric or magnetic circuit and thermal demagnetization from the operating temperature. In this sense, cobalt-ferrite (CoFe$_2$O$_4$) is one of the most promising materials because of its high magnetic anisotropy among ferrites,[5] so effective processing methods are demanded.

CoFe$_2$O$_4$ is an inverse spinel ferrite with most of Co^{2+} ions occupying octahedral sites (B sites) and the Fe^{3+} ions on both tetrahedral (A sites) and octahedral sites. Many synthesis techniques have been successfully applied to obtain the spinel phase of CoFe$_2$O$_4$, such as the hydrothermal method,[6,7] microwave calcination,[8] sol-gel process,[9,10] thermal decomposition,[11,12] and co-precipitation technique.[13] Among these techniques the co-precipitation route offers the possibility of easy scalability and cost-efficiency under proper optimization of the preparation parameters. Coercivity in cobalt ferrite can be enhanced by controlling the particle size distribution and by inducing high level residual strain through mechanical milling. For instance, CoFe$_2$O$_4$ powders after milling for 1.5 hours have shown record values of coercivity of about 5.1 kOe and an energy product, $(BH)_{max} = 15.9$ kJ m^{-3} at room temperature (RT).[14] This enhancement is probably due to the stress anisotropy and defects created during

[a] Division of Permanent Magnets and Applications, IMDEA-Nanociencia, Campus Universidad Autónoma de Madrid, 28049 Madrid, Spain, E-mail: Alberto.Bollero@imdea.org
[b] Departamento de Física de la Materia Condensada and Instituto "Nicolás Cabrera", Universidad Autónoma de Madrid, 28049 Madrid, Spain.

RSC Advances Accepted Manuscript

processing, which might act as pinning centers during magnetization reversal.[15] A milling time of 1.5 hours is a significant advance by comparison with typical durations of dozen of hours, but still excessively long to consider its implementation in permanent magnets manufacture plants. Furthermore, and from a scientific point of view, a detailed and systematic study that might allow for discrimination of the different parameters involved in the mechanism for increased coercivity, i.e., a proper understanding of the mechanisms involved in coercivity development, is still missed in the literature.

In this Letter we provide a detailed and systematic study on Co-ferrite powders synthetized by co-precipitation with tailored properties via ultrafast ball-milling and heating procedures. In particular, morphology, microstucture, and magnetic properties are discussed as a function of milling time and heating temperature, providing a comprehensive correlation between them, in order to produce high performance isotropic Co-ferrites with energy products up to 17.8 kJ m^{-3} at room temperature. Furthermore, this efficient methodology provides a technological key to manage the production of isotropic powders in processing times of only a few minutes. The combination of high performance isotropic Co-ferrite powders with feasible scalable synthesis and processing method in record time make them good candidates for rare-earth free permanent magnet applications.

2 Experimental

2.1 Chemicals

Commercial products iron(III) chloride hexahydrate ($\geq$ 98%, Sigma-Aldrich), cobalt(II) chloride hexahydrate ($\geq$ 98%, Sigma-Aldrich), ammonium hydroxide solution (25% in water, Sigma-Aldrich), were used as received.

2.2 Synthesis of cobalt ferrite

Starting Co-ferrite was synthesized by conventional co-precipitation method. A solution of $CoCl_2 \cdot 6H_2O$ (11.9 g, 0.05 mol) in distilled water (200 ml) was added to another solution of $FeCl_3 \cdot 6H_2O$ (27 g, 0.10 mol) in distilled water (200 ml) as well. The solution was heated to 77 °C under vigorous magnetic stirring. Then, 75 ml of NH_4OH (25% in water) were added and a black precipitate was formed immediately. The mixture was kept at 77 °C for 30 minutes under stirring and then allowed to cool down to room temperature. Once the powder was settled on the bottom of the recipient, the liquid phase was separated from the precipitate with the aid of a water pump, and the remaining black solid was washed three times with distilled water (3 x 500 mL) following the same procedure. Finally, the solid was redispersed in water (500 mL) and the particles were separated by centrifugating at 9000rpm during 5 minutes with water (2 x 250 mL) and acetone (1 x 250 mL). After this process, the sample was heated at 80 °C during 12 hours to allow the evaporation of the liquid phase, resulting in a brown powder.

The powder resulting from the synthesis was annealed during 1 hour at 1000 °C to crystallize the inverse spinel structure of $CoFe_2O_4$. High-energy ball milling experiments with a total duration of 30, 60, 90, 120 and 180 seconds were performed on 4
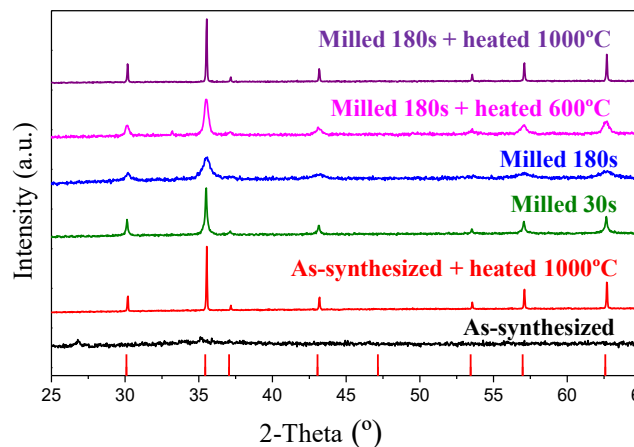

Fig. 1 XRD spectra of $CoFe_2O_4$ powders. From bottom to top: as-synthesized, as-synthesized after heating at 1000°C (starting), milled (30 and 180 sec), and heated at 600 and 1000 °C after milling (180 sec). Reference lines correspond to $CoFe_2O_4$ (Ref. 00-022-1086).

grams of the aforementioned $CoFe_2O_4$ using a high-energy ball milling equipment at a speed of 900 rpm with a ball-to-powder ratio of 40:1. Tungsten carbide milling media (balls and vessel) have been used to enhance the impact energy, i.e. accelerate an efficient milling process, due to the larger density (14.95 g/cm^3) by comparison with that of steel (7.8 g/cm^3). The effect of post-heating temperature on magnetic properties of $CoFe_2O_4$ powders milled for 180 seconds was assessed by heating in the temperature range of 400-1000 °C using air atmosphere in a Carbolite tubular oven model STF 15/450. The heating procedure consisted on an increasing temperature ramp of 10K/min from room temperature to the goal temperature which was maintained for 1 hour before cooling down to room temperature.

2.3 Characterization

X-Ray diffraction (XRD) spectra were measured with a Highscore X'pert θ-2θ diffractometer, with Cu-K_α radiation source. Mean crystallite size was calculated from the most intense peaks of the measured XRD spectra using the Scherrer law,[16] and the quantification of residual strain was obtained from a Williamson-Hall analysis.[17] Scanning electron microscopy (SEM) data were used to obtain microstructural and morphological information, using a Carl-Zeiss Auriga microscope at a filament voltage of 3 kV. Magnetization *M-H* curves were measured at room temperature with a Lakeshore 7400 vibrating sample magnetometer (VSM). The parameters extracted from the loops include magnetization at maximum applied field of 20 kOe (M_{20kOe}), remanence (M_r), and coercivity (H_c). $(BH)_{max}$ has been evaluated, in order to quantify the performance as permanent magnets and to assess the suitability of our methodology.

3 Results and discussion

3.1 X-ray diffraction

Representative XRD patterns are shown on Figure 1. The diffractogram of the starting product of the co-precipitation reaction shows broad and unresolved peaks as the synthesis of well de-

fined $CoFe_2O_4$ nanoparticles usually requires higher temperatures in accordance to previous reports.[18–20] Once the sample is annealed at 1000 °C or post-processed (milled and annealed after milling) powders show just reflection peaks corresponding to $CoFe_2O_4$ phase, indicating the absence of any other phase or possible contamination during the milling and heating process. Milling for 30 and 180 s results in a progressive broadening of the reflection peaks due to refinement of the microstructure. Subsequent heating treatments at 600 and 1000 °C lead to narrower peaks with increasing temperature indicative of the progressive grain growth.

The parameters extracted from XRD data are analyzed as a function of milling time and post-milling heating temperature. Figure 2(a) display the evolution of the values for the mean crystallite size and the microstrain of the starting and the as-milled materials. The estimated average crystallite size of the starting powder is 117.6 nm, which is reduced down one order of magnitude to 15.9 nm after only 90 seconds of milling, well below the $CoFe_2O_4$ monodomain regime (40 nm).[21] The mean crystallite size after 180 seconds milling is 9.1 nm. Positive sign of calculated strains indicates a tensile strain induced during mechanical milling, increasing from $0.5 \; 10^{-3}$ for the starting material prior to milling to $9 \; 10^{-3}$ after milling for 180 seconds. Post-milling heat treatment causes a recrystallization of $CoFe_2O_4$ powders followed by grain growth effects. The evolution of the powder mean crystallite size and residual strain as a function of the post-milling heating temperature is plotted in Figure 2(b). The mean grain size increases with increasing the heating temperature, from 13.4 to 114.2 nm for powders heated in the range 400-1000 °C, respectively. It turns, the post-milling heating process results in a relaxation of the strain induced during milling with a dramatical decrease from $6.1 \; 10^{-3}$ to $0.7 \; 10^{-3}$, for powders heated from 400 to 1000 °C, respectively.

3.2 Microstructural analysis

The microstructure of powders can be visualized in Figure 3, for different milling times (left images) and heat treatments (right). It is clearly observed in inset of Figure 3(a) that the starting powder is constituted by polycrystalline micron-size particles with well-defined crystals, as it has been reported previously for sintered $CoFe_2O_4$ material.[22] The efficiency of this ultrafast milling method in obtaining a refined and homogeneous powder in a short milling time is evidenced when comparing particle size of the starting material (Figure 3(a)) with that obtained after 30 and 180 seconds of milling (Figs. 3(b) and 3(c), respectively). SEM images obtained for powders milled for 30 seconds (Figure 3(b)) demonstrates the coexistence of particles with two different size distributions; such a short milling time is not sufficient to refine homogeneously the microstructure, resulting in a mixture of remaining micron-size particles in addition to newly created particles in the submicrometer regime. Homogenization of the material is guaranteed through extended milling time of 180 s (Fig. 3(c)).

Aggregates of submicrometer particles are observed in more detail in inset of Fig. 3(f). SEM images included in Figures
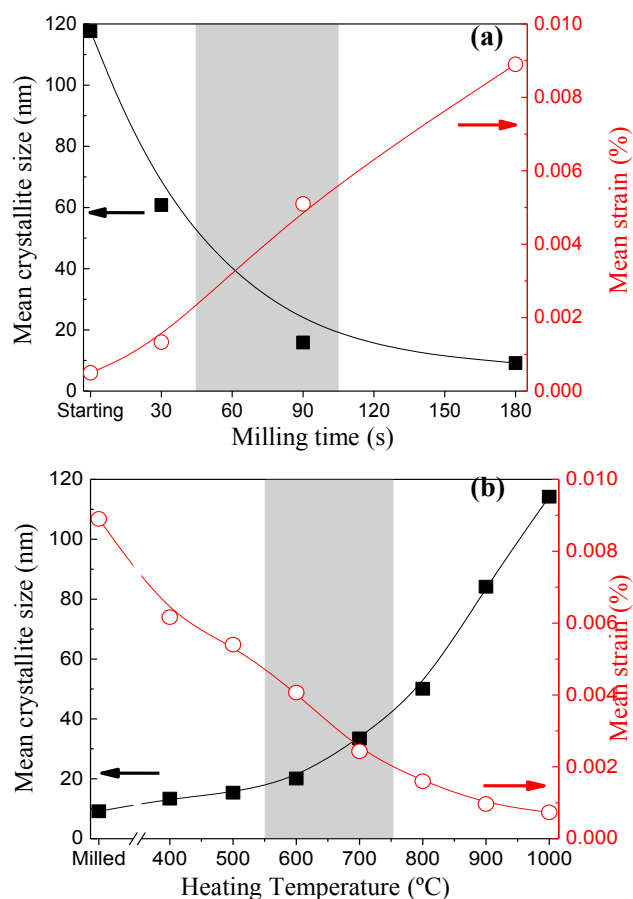

Fig. 2 Evolution of grain size (filled symbols) and residual strain (empty circles) with (a) milling time, and (b) heating temperature for the 180 seconds milled sample. Lines are guides for the eye. Shadowed areas highlight the regions with the best combination of magnetic properties (see Fig. 5).

3(d-f) show the microstructure of this latter sample after heating at different temperatures. The images do not allow to observe significant differences neither in morphology nor in particle size by increasing the heating temperature from 400 to 600 °C (Figs 3(d) and 3(e), respectively). By comparison, heating at 1000 °C results in significantly enlarged particles with polyhedral shapes typical of sintered metallic materials.

3.3 Magnetic properties

Room-temperature magnetization curves of the starting $CoFe_2O_4$ powder and after different milling times are represented in Figure 4(a). At a first glance, there is a strong increase in coercivity with increasing the milling time accompanied by a change in the shape of the hysteresis loop. The two-steps hysteresis loop measured after milling for 30 seconds is characteristic of a magnetic material with an inhomogeneous microstructure consisting of particles with a broad particle size distribution. This is in good agreement with SEM observations (Fig. 3(b)) where large (up to $10\mu m$) and small (nanometric) particles are observed. Milling for 90 s leads to a single hysteresis loop (Fig. 4(a)) while 180 s is sufficient to homogenize the microstructure (Fig. 3(f)) resulting in a more
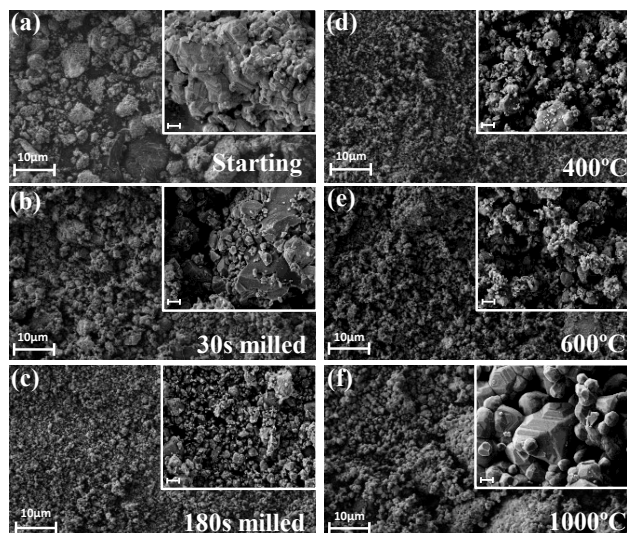
Fig. 3 SEM images of CoFe$_2$O$_4$ powders. (a) starting; (b)-(c) after different milling times;(d)-(f) after heating at different temperatures the 180 s milled powder. Scale bar: 10 μm. Insets: Magnified images (scale bar: 500 nm).
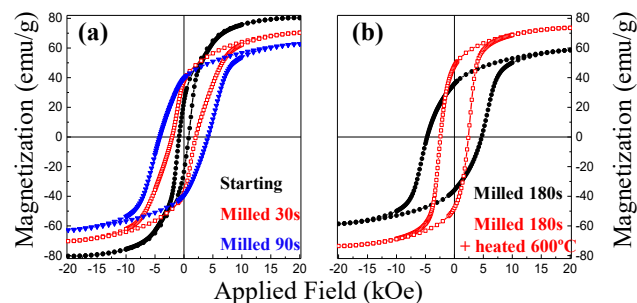

Fig. 4 Hysteresis loops evolution of CoFe$_2$O$_4$ powders (a) after milling with different milling times; and (b) after heating at different temperatures the 180 s milled powder.

defined squareness of the hysteresis loop (Fig. 4(b)). Subsequent heating of this milled powder at 600 °C reduces coercivity in favor of enhanced remanence and saturation magnetization (Fig. 4(b)). The influence of heating on the magnetic properties of milled powders is discussed in detail in the following.

The evolutions of the magnetic properties as a function of milling time and heating temperature are shown in Figs. 5(a) and 5(b), respectively. Milling for 90 s is sufficient to achieve a coercivity well above 4 kOe (Fig. 5(a)) while extending this milling time to 180 s results in a 5.5 times increase in H_c from 0.83 kOe for the starting material to 4.7 kOe for the as-milled powder. This large increase in coercivity is the combined result of a reduced mean crystallite size and the induced strain during milling (Fig. 2(a)) that results in the creation of defects acting as pinning centers during magnetization reversal. It is important to highlight that while other studies present same trend of increasing coercivity with increasing milling time,[23] we have reduced the timescale of the process from several hours to a few minutes. Furthermore, and by using this extremely short processing time, we have managed to obtain the best combination of magnetic properties (H_c=4.7 kOe, M_r=35.8 emu/g) reported in literature for high coercive Co-ferrite powders, with $(BH)_{max}$ = 10.4 kJm^{-3}. Magnetization M_{20kOe} decreases with extended milling times, decreasing from 80.0 emu/g for the initial powder to 62.5 emu/g after milling for 180 seconds. This observation can be explained as an effect of surface-to-volume ratio modification due the size reduction undergone on initial micronsize particles as well as its partial amorphization during extended milling. An increased surface-to-volume ratio will evidence the effect of the "dead layer" (due to spin disorder in a surface shell region contributing less to the magnetization than the core due to spin fluctuations at the surface) originating the decrease in M_{20kOe} and M_r.[24,25] Interestingly, and contrary to the trend followed by M_{20kOe}, M_r increases from 23.5 emu/g for the starting material

(defined in the following as synthesized by co-precipitation and heated at 1000 °C) to 37.7 and 39.9 emu/g after milling for 30 and 60 s, respectively, prior to a parallel decrease of M_{20kOe} for longer milling times. A extremely short milling time (< 60 s) is not sufficient for amorphization of the material but it is indeed sufficient to diminish particle and grain size and approach the monodomain regime. A maximum of $(BH)_{max}$=12.8 kJm^{-3} is attained after milling for 60 s. Milling time up to 180 s keeps increasing coercivity, but the progressive decrease in magnetization results in reduced $(BH)_{max}$. Longer milling times display as well a coercivity reduction, similar to previous studies[14], resulting thus detrimental for $(BH)_{max}$.

Tuning of the magnetic properties and $(BH)_{max}$ enhancement of the high coercive Co-ferrite powders is possible by subsequent heating of the as-milled powders in air. Figure 5(b) shows the evolution of magnetic properties for powders resulting from milling for 180 seconds followed by heat treatment in the temperature range 400-1000 °C. As a first observation, heating of the as-milled powders results in an increase of M_{20kOe} due to crystallization of the amorphous phase and grain growth effect observed with increasing temperature (Fig. 1). On the other hand, and by comparison with the stepped increase in coercivity previously obtained for the powders with increasing milling time (Fig. 5(a)), a post-heat treatment strongly degrades the attained coercivity (Fig. 5(b)). As a clear example, post-heat treatment at 600 °C results in an enlarged remanence M_r=47.5 emu/g and a coercivity H_c=2.4 kOe, which is the half of the coercivity obtained for the starting as-milled material. A further increased temperature of 1000 °C leads to a reduced H_c=1.2 kOe. This behavior is due to the combined effect of the increased mean crystallite size -evolving from the monodomain (below 40 nm for T $\leq$ 700 °C) to the multidomain regime- in combination with relaxation of the strain induced during milling (Fig. 2(b)). However, the latter is playing a predominant role as proven by the fact that crystallite size does not vary significantly in the temperature range 400-700 °C while the mean strain drops, and accordingly the measured coercivity decreases dramatically from 4.7 to 2.1 kOe after heating at 400 and 700 °C, respectively. An increased heating temperature results in a progressive elimination of the defects that were acting as pining centers for magnetization reversal in the as-milled powders, i.e. consequently decreasing coercivity. Heating above 800 °C affects the microstructure due to a con-

siderable particle size growth (Fig. 3), and in this case, coercivity only decreases from 1.9 to 1.2 kOe after heating the milled sample at 800 and 1000 °C, respectively. The combination of an optimum remanence magnetization and a still significant coercivity obtained in the range 600-700 °C results in a maximum $(BH)_{max}$ =17.8 kJm^{-3} well above the value determined for the as-milled powders. This value compares to the state-of-the-art value of 18 kJm^{-3}, reported for Co-ferrite nanoparticles synthesized by thermal decomposition of metal-organic precursors.[5] The advantage of the here proposed method is the possibility of producing large amounts of material with extremely short processing times. It is interesting to note that heating of the as-milled powder at 1000 °C results in practically complete reversibility in microstructural (Fig. 2) and magnetic properties (Fig. 5), i.e. obtaining values comparable to those measured for the starting material prior to milling.
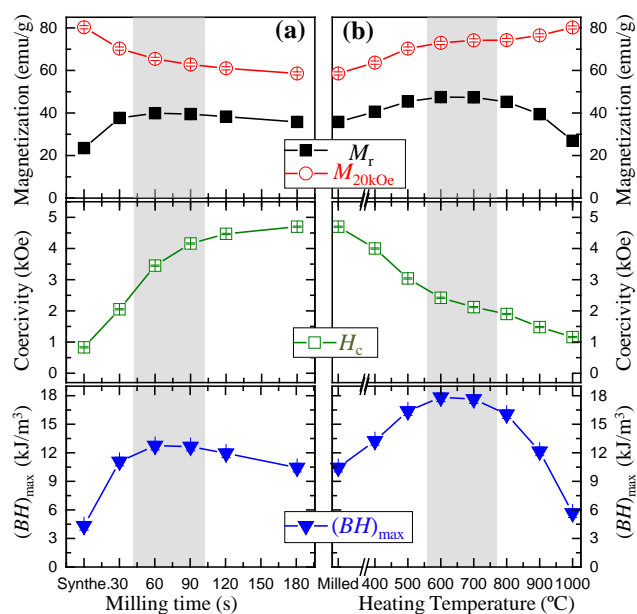

Fig. 5 Evolution of magnetic properties of CoFe$_2$O$_4$ powders with (a) milling time and (b) heating temperature. Lines are guides for the eye. The regions with the best combination of magnetic properties are marked by shadowed areas.

Therefore the study has a proven double functionality by allowing, first, gaining insight in the influence of grain size and strain relaxation in the coercivity mechanism in milled Co-ferrite powders. Secondly, it has allowed the right choice of processing parameters (milling time and processing temperature) to maximize $(BH)_{max}$ at room temperature. From all experimental data, the best performance regarding $(BH)_{max}$ is linked to a compliance between nanostructuration and microstrain.

4 Conclusions

In conclusion this study has shown the possibility of achieving a 5-fold increase in coercivity in CoFe$_2$O$_4$ powders, with a maximum value of 4.7 kOe obtained after milling for 180 seconds. Therefore, the timescale of the process has been reduced from several hours typically used to a 3 minutes. The fundamental role played by microstrain induced during milling in increasing the coercivity has been discriminated from grain size effects. This understanding has allowed the right choice of processing parameters (milling time and processing temperature) to obtain a $(BH)_{max}$ = 17.8 kJm^{-3} in powders milled for 180s and heated at 600 °C. This combination of magnetic properties obtained for isotropic CoFe$_2$O$_4$ powders with effective processing times and feasible scalable synthesis methods (co-precipitation and ultrafast milling), make them good candidates for permanent magnet applications.

Acknowledgements

References

1 O. Gutfleisch, M.A. Willard, E. Brück, C.H. Chen, S.G. Sankar and J. Ping Liu, *Adv. Mater.*, 2011, **23**, 821-842.

2 L.H. Lewis and F. Jiménez-Villacorta, *Metall. Mater. Trans.*, 2011, A **44**, 2.

3 K.H.J. Buschow and F.R. de Boer, *Physics of Magnetism and Magnetic Materials*, 2003, (Kluwer Academic, New York) Chapter 12

4 A. Goldman, *Modern Ferrite Technology*, 2006, (Springer, Pittsburgh) Chapter 9.

5 A. López-Ortega, E. Lottini, C. de Julian Fernández and C. Sangregorio, *Chem. Mater.*, 2015, **27**, 4048-4056.

6 F. Zhang, R. Su, L. Shi, Y. Liu, T. Chen and Z. Wang, *Advanced Materials Research*, 2013, Vols. 821-822, pp 1358-1361.

7 H.L. Andersen and M. Christensen, *Nanoscale*, 2015, **7**, 3481.

8 A.M. Ibrahim, M.M. Abd El-Latif and M.M. Mahmoud, *J. Alloys Compd.*, 2010, **506**, 201-204.

9 A. Hunyek, C. Sirisathitkul and P. Harding, *Advanced Materials Research, Vols.*, 2010, **93-94**, pp 659-663.

10 A. Quesada, C. Granados-Miralles, A. López-Ortega, S. Erokhin, E. Lottini, F.J. Pedrosa, A. Bollero, A.M. Aragón, F. Rubio-Marcos, M. Stingaciu, G. Bertoni, C. de Julián Fernández and C. Sangregorio, J.F. Fernández, D. Berkov and M. Christensen, *Adv. Electron. Mater.*, 2016, **2**, 1500365.

11 S. Prasad, A. Vijayalakshmi and N.S. Gujbhiye, *J. Thermal Anal. Vol.*, 1998, **52**, 595-607.

12 Le T. Lu, Ngo T. Dung, Le D. Tung, Cao T. Thanh, Ong K. Quy, Nguyen V. Chuc, Shinya Maenosono and Nguyen T. K. Thanh, *Nanoscale*, 2015, **7**, 19596-19610.

13 Y. Zhang, Z. Yang, D. Yin, Y. Liu, C. Fei, R. Xiong, J. Shi and G. Yan, *J. Magn. Magn. Mater.*, 2010, **322**, 3470-3475.

14 B.H. Liu and J. Ding, *Appl. Phys. Lett.*, 2006, **88**, 042506.

15 B.H. Liu, J. Ding, Z.L. Dong, C.B. Boothroyd, J.H. Yin and J.B. Yi, *Phys. Rev. B*, 2006, **74**, 184427.

16 A.L. Patterson, *Phys. Rev.*, 1939, **56** (10): 978-982.

17 G.K. Williamson and W.H. Hall, *Acta Metall.*, 1953, **1**, 22.

18 F. A. Tourinho, R. Franck and R. Massart, *J. Mater. Sci.*, 1990, **25**, 3249-3254.

19 Y. I. Kim, D. Kim and C. S. Lee, *Physica B*, 2003, **337**, 42-51.

20]D. Moitra, S. Hazra, B. K. Ghosh, R. K. Jani, M. K. Patra, S. R. Vadera and N. N. Ghosh, *RSC Adv.*, 2015, **5**, 51130-51134.

21 C.N. Chinnasamy, B. Jeyadevan, K. Shinoda, K. Tohji, D.J. Djayaprawira, M. Takashi, R. Justin Joseyphus and A.Narayanasamy, *Appl. Phys. Lett.*, 2003, **83**, 2862.

22 W.S. Chiu, S. Radiman, R. Abs-Shukor, M.H. Abdullah and P.S. Khiew, *J. Alloys Compd.*, 2008, **459**, 291-297.

23 A.S. Ponce, E.F. Chagas, R.J. Prado, C.H.M. Fernandes, A.J. Tejero and E. Baggio-Saitovitch, *J. Magn. Magn. Mater.*, 2013, **344**, 182-187.

24 E. Swatsitang, S. Phokha, S. Hunpratub, B. Usher, A. Bootchanont, S. Maensiri and P. Chindaprasirt, *J. Alloys Compd.*, 2016, **664**, 792-797.

25 A. Franco Jr, F.C. e Silva and V.S. Zapf, *J. Appl. Phys.*, 2012, **111**, 07B530.

RSC Advances Accepted Manuscript